15-Deoxy-$\Delta^{12,14}$-prostaglandin J_2 inhibits migration of human thyroid carcinoma cells by disrupting focal adhesion complex and adherens junction

YA-CHIEH WU[1], YUN-TING JHAO[2], YU-CHEN CHENG[3] and YING CHEN[3,4]

[1]Department of Nursing, Ching Kuo Institute of Management and Health, Keelung 203; Graduate Institute of [2]Medical and [3]Life Sciences; [4]Department of Biology and Anatomy, National Defense Medical Center, Neihu, Taipei 114, Taiwan, R.O.C.

Received August 17, 2015; Accepted November 28, 2016

DOI: 10.3892/ol.2017.5773

Abstract. Metastasis is frequently observed in human follicular thyroid carcinoma. The present study investigated the peroxisome proliferator-activated receptor γ agonist, 15-deoxy-$\Delta^{12,14}$-prostaglandin J^2 (15d-PGJ_2), and its effect on the migration of CGTH W-2 human thyroid carcinoma cells. 15d-PGJ_2 decreased the survival rate of CGTH W-2 cells in a dose-dependent manner. The Transwell migration assay demonstrated that 15d-PGJ_2 reduced the migration rate of CGTH W-2 cells by 35% following treatment with 30 μM 15d-PGJ_2 compared with control cells. The cell adhesion assay indicated that, following 15d-PGJ_2 treatment for 24 h, cell adhesion decreased by 26% compared with the control group. The expression levels of focal adhesion proteins, including integrin β1, phospho-focal adhesion kinase and p-paxillin, were downregulated following treatment with 15d-PGJ_2. Immunostaining revealed that the puncta of vinculin were reduced and the actin stress fiber was disassembled following 15d-PGJ_2 treatment. By contrast, p120-catenin (p120-ctn) and β-catenin levels staining accumulated in the region of the lamellipodium following 15d-PGJ_2 treatment. Membrane fractionation revealed that p120-ctn and N-cadherin were decreased in the cell membrane, but increased in the cytoplasm of 15d-PGJ_2-treated cells. Therefore, 15d-PGJ_2 inhibited human thyroid carcinoma cell migration and this may be due to the impairment of focal adhesion complexes and the accumulation of p120-ctn in the cytoplasm in the region of the lamellipodium.

Correspondence to: Mrs. Ying Chen, Department of Biology and Anatomy, National Defense Medical Center, 161, Section 6, Minquan East Road, Neihu, Taipei 114, Taiwan, R.O.C.
E-mail: ychen0523@mail.ndmctsgh.edu.tw

Key words: 15-deoxy-$\Delta^{12,14}$-prostaglandin J_2, thyroid carcinoma, migration, adherens junction, focal adhesion complex

Introduction

Thyroid carcinoma was identified as one of the 5 most prevalent types of cancer developing in females from Taiwan, and thyroid carcinoma is a common type of endocrine malignancy (1). The majority of thyroid carcinomas are differentiated thyroid carcinomas, which include follicular and papillary subtypes (2). Lung and bone metastases are frequently observed in follicular thyroid carcinoma (3), and the increase of pair box 8-peroxisome proliferator-activated receptor γ (PPARγ) fusion proteins, which inhibit the normal function of PPARγ, is common in thyroid carcinoma (4). Low expression levels of PPARγ are correlated with poor thyroid tumor differentiation and higher proliferative activity (5). Additionally, activation of PPARγ inhibits cancer cell growth in follicular and anaplastic thyroid carcinoma cells (6). PPARγ agonists have been reported to reverse the process of the epithelial-mesenchymal transition (EMT) and reduce the migration of thyroid cancer cells (7). In anaplastic and follicular thyroid carcinoma cells, N-cadherin replaces the role of E-cadherin and exhibits functionality as part of N-cadherin/β-catenin complexes (8). However, the mechanisms underlying the effects of PPARγ on cell migration and the role of N-cadherin in thyroid carcinoma cells require further study.

The loss of cell-cell adhesion and the decreased number of cell-matrix junctions promotes cancer cell migration and invasion (9). The EMT is a major pathologic cause of tumor malignancy and is usually accompanied by the loss of E-cadherin (10). Follicular and anaplastic thyroid carcinoma cells that lack E-cadherin expression, instead expressing N-cadherin, may contribute to the formation of cadherin/catenin complexes that promote tumor migration and invasion (11,12). Catenins are armadillo-family proteins, including α-, β-, γ- and p120-catenins, that serve an important role in bridging cadherin to microfilaments (13). A previous study reported that p120-catenin (p120-ctn) regulates cell motility through the reduction of Rho GTPase activity (14). The PPARγ agonists, pioglitazone and rosiglitazone, inhibit cell growth and invasion via blocking β-catenin (β-ctn) in human glioma cells and colorectal cancer cells, respectively (15,16). The role of adherens junctions in the action of PPARγ agonists in thyroid carcinoma cells remains to be elucidated.

The remodeling of cell-matrix junctions by the integrin-regulated signaling pathway and focal adhesion complexes contribute to tumor cell migration and invasion (17). The focal adhesion complex proteins include focal adhesion kinase (FAK), Src, paxillin, talin and vinculin (18). FAK controls cell migration and invasion through overexpression or activation by Src, which phosphorylates FAK (19). A previous study reported that the PPARγ agonists ciglitazone and 15-deoxy-$\Delta^{12,14}$-prostaglandin J_2 (15d-PGJ$_2$) induced apoptosis and reduced FAK and paxillin phosphorylation, in human thyroid carcinoma cells (20). The current study further investigates the effects of PPARγ agonist on cell migration in metastatic thyroid carcinoma.

Materials and methods

Cell culture. The CGTH W-2 cell line is derived from metastatic thyroid follicular carcinoma from a Chinese patient in Taiwan, and was a gift from Dr Jen-Der Lin (21). The cells have a doubling time of 18 h and have lost the majority of their iodine-concentrating ability and the capacity for thyroglobulin synthesis. The cells were grown in RPMI-1640 supplemented with 10% fetal bovine serum (FBS), 1 mM sodium pyruvate, 100 IU/ml of penicillin and streptomycin (Gibco; Thermo Fisher Scientific, Inc., Waltham, MA, USA) in a humidified atmosphere containing 5% CO_2 at 37˚C. The rat fibroblasts were minced in Ca^{2+}/Mg^{2+}-free Hank's balanced salt solution from ventricles (HBSS; Gibco; Thermo Fisher Scientific, Inc.), then incubated for 15 min at 37˚C with a mixture of 0.5 mg/ml of collagenase type II (Sigma-Aldrich; Merck Millipore, Darmstadt, Germany) and 0.6 mg/ml of pancreatin (Sigma-Aldrich; Merck Millipore) in HBSS. The digestion was repeated a further 2 times with fresh enzyme mixture, then the combined cell suspensions from the digestions were mixed with an equal volume of ice-cold plating medium consisting of minimal essential medium (Gibco; Thermo Fisher Scientific, Inc.) containing 10% FBS, 100 IU/ml of penicillin, and 100 µg/ml of streptomycin (Gibco; Thermo Fisher Scientific, Inc.), and centrifuged at 1,000 x *g* for 10 min at room temperature, then the cells were resuspended in plating medium for 1 h at 37˚C to collect fibroblasts.

Cell survival assay. Thyroid carcinoma cells were plated at 2x10^4 cell/well in 24-well plates and cultured for 24 h at 37˚C with 10, 20, 30, 40 and 60 µM 15d-PGJ$_2$ (Sigma-Aldrich) in the presence of 10% FBS prior to assaying for cell viability. Following two washes with PBS (137 mM NaCl, 2.7 mM KCl, 1.5 mM KH_2PO_4, 8 mM Na_2HPO_4; pH 7.4), 500 µl RPMI containing 0.5 mg/ml MTT reagent (Sigma-Aldrich; Merck Millipore) was added to each well, then incubation was continued for 4 h at 37˚C to allow the conversion of the substrate into purple formazan product. The medium was removed and the cells were lysed with dimethyl sulfoxide (DMSO) and the absorbance was measured at a wavelength of 590 nm measured by a spectrophotometer (Beckman Coulter, Inc., Brea, CA, USA).

Apoptosis assay. The CGTH W-2 cells were treated with DMSO or 30 mM 15d-PGJ$_2$ for 24 h at 37˚C, washed with PBS and fixed for 5 min in 5% formalin and 0.5% Triton X-100 at room temperature. The cells were washed with PBS, stained for 15 min at room temperature with 1 µg/ml DAPI (Sigma-Aldrich; Merck Millipore) in 0.9% NaCl and mounted using mounting medium (Sigma-Aldrich; Merck Millipore). Apoptotic cells were identified using the presence of chromatin condensation or apoptotic body formation by a Zeiss epifluorescence microscope (Carl Zeiss AG, Oberkochen, Germany) equipped with a Nikon DIX digital camera (Nikon Corporation, Tokyo, Japan). All experiments were performed in triplicate and >100 cells were examined.

Transwell assay. To determine migratory ability, 1x10^5 CGTH W-2 cells were seeded in the upper chamber of a Transwell apparatus with an 8 mm pore polycarbonate membrane (Costar®; Corning Incorporated, Corning, NY, USA). Following cell attachment, the cells were cultured in growth medium, with or without 30 mM 15d-PGJ$_2$ (Enzo Life Sciences, Inc., Farmingdale, NY, USA), for 24 h at 37˚C. Following removal of the cells on the upper side of the polycarbonate membrane using a cotton swab, the cells on the lower side were fixed for 10 min in 10% formalin and stained for 5 min at room temperature with Coomassie brilliant blue G250 (Sigma-Aldrich; Merck Millipore). The numbers of migrated cells were imaged using an upright bright-field microscope (Nikon Corporation) and analyzed by ImageJ (version 1.64r; National Institutes of Health, Bethesda, MD, USA) in 3 randomly selected fields for each membrane and triplicate membranes examined for each experimental group.

Wound healing assay. The CGTH W-2 cells were grown to confluence as monolayer. The cells were scratched using a P200 pipette tip and imaged as previously described (22). Following 24 h treatment with DMSO or 30 mM 15d-PGJ$_2$ at 37˚C, the wound healing was imaged using an upright bright-field microscope (Nikon Corporation) and analyzed by ImageJ. Images are representative of three separate experiments.

Adhesion assay. Following treatment with DMSO (control) or 30 µM 15d-PGJ$_2$ at 37˚C, CGTH W-2 cells were suspended and plated on fibronectin-coated or non-coated dishes as described previously (11). The cells were allowed to adhere for 15 min at 37˚C and the medium and non-adhered cells were subsequently discarded. Following PBS washes, the adhered cells were examined using an inverted bright-field microscope (Nikon Corporation) and the number of cells in 3 random fields were counted.

Immunofluorescence microscopy. Following DMSO or 30 µM 15d-PGJ$_2$ treatment at 37˚C, the CGTH W-2 cells were washed with PBS, then fixed for 5 min with 10% formalin in PBS and permeabilized for 10 min with 0.1% Triton X-100 in PBS at room temperature. Following the PBS washes (3 times for 5 min each), nonspecific binding was blocked with a 30 min incubation at room temperature with 5% non-fat milk in PBS. The cells were incubated overnight at 4˚C with monoclonal mouse antibodies against p120-ctn (dilution, 1:100; cat. no., 610133) or β-ctn (dilution, 1:100; cat. no., 610153; BD Biosciences, Franklin Lakes, NJ, USA), or vinculin (dilution, 1:100; cat. no., V4505; Sigma-Aldrich; Merck Millipore) washed with PBS and incubated for 1 h at 37˚C with fluorescein isothiocyanate (FITC)-conjugated secondary antibodies (dilution, 1:50;

cat. no., 715-095-151; Jackson ImmunoResearch Laboratories, Inc., West Grove, PA, USA). For F-actin labeling, the cells were incubated with FITC-phalloidin (dilution, 1:100; cat. no., P5282; Sigma-Aldrich; Merck Millipore). Finally, the cells were washed with PBS, mounted with Gel Mount™ Aqueous mounting medium (Sigma-Aldrich; Merck Millipore) and detected using a fluorescent microscope (DM2500; Leica Microsystems GmbH, Wetzlar, Germany) and images were captured using a Nikon D1X digital camera (Nikon Corporation, Tokyo, Japan).

Western blotting. Following DMSO or 30 μM 15d-PGJ_2 treatment for 24 h at 37˚C, CGTH W-2 thyroid carcinoma cells were washed with PBS and homogenized in lysis buffer for 10 min at 4˚C (10 mM ethyleneglycoltetraaceticacid, 2 mM $MgCl_2$, 60 mM piperazine-N,N'-bis(2-ethanesulforic acid), 25 mM 4-(2-hydroxethyl)-1-piperazineethanesulfonic acid, 0.15% Triton X-100, 1 μg/ml pepstatin A, 1 μg/ml leupeptin, 1 mM NaF and 1 mM phenylmethylsulfonyl fluoride). Subsequently an equal volume of sample buffer (0.25% bromophenol blue, 0.5 M dithiothreitol, 50% glycerol, 10% SDS) was added and the mixture was heated at 90˚C for 3 min. Proteins (60 μg per lane) were electrophoresed by 10% SDS-PAGE and transferred to a nitrocellulose membrane (Bio-Rad Laboratories, Inc., Hercules, CA, USA). Strips from the membrane were blocked by incubating for 30 min at room temperature with 5% non-fat milk in TBS (pH 8.2) containing 0.1% Tween (TBST) and incubated overnight at 4˚C with a 1:1,000 dilution of monoclonal mouse antibodies against integrin β1 (cat. no., 610467), FAK (cat. no., 610087), paxillin (cat. no., 610051), N-cad (cat. no., 610920), p120-ctn (cat. no., 610133; BD Biosciences), vinculin (cat. no., V4505) or β-actin (cat. no., A3854; Sigma-Aldrich; Merck Millipore), or a 1:500 dilution of rabbit antibodies against phosphorylated FAK (cat. no., 44-624G), phosphorylated paxillin (cat. no., 44-720G; Thermo Fisher Scientific, Inc.) and a 1:1,000 dilution of GAPDH (cat. no., 2251-1), Na^+/K^+ ATPase (cat. no., 2047-1; Epitomics, Burlingame, CA, USA) in TBST. Following TBST washes, the strips were incubated for 2 h at room temperature with 1:7,500 dilution of alkaline phosphatase-conjugated anti-mouse (cat no., S3721) or anti-rabbit immunoglobulin G antibodies (cat. no., S3731; Promega Corporation, Madison, WI, USA) and bound antibody was visualized using nitro blue tetrazolium and 5-bromo-4-chloro-3-indolyl phosphate (Sigma-Aldrich; Merck Millipore) as the chromogen. The density of the bands on the nitrocellulose membrane was quantified with densitometry using Gel Pro 3.1 (Media Cybernetics, Inc., Rockville, MD, USA). The density of the band in the control sample was taken as 100% and the density of the band in the test sample was expressed as a percentage of the control density. All the experiments were performed ≥3 times and the data are expressed as the mean ± standard deviation.

Membrane fractionation. Following treatment with DMSO or 30 μM 15d-PGJ_2 for 24 h at 37˚C, CGTH W-2 thyroid carcinoma cells were washed with PBS and ultrasonicated for 2 periods of 10 sec in immunoprecipitation buffer (50 mM Tris-HCl, 1% Triton X-100, 0.25% sodium deoxycholate, 150 mM NaCl, 1 mM EDTA, 1 mM phenylmethylsulfonyl fluoride, 1 mM NaF, 1 mM Na_3VO_4, 1 mg/ml each of aprotinin, leupeptin and pepstatin; pH 7.4). The suspension was centrifuged at 20,000 x *g* for 30 min at 4˚C and the supernatant was used as the Triton-soluble portion. Membrane and cytosolic fractions of cell lysates were analyzed for N-cadherin and p120-ctn expression using western blotting following 15d-PGJ_2 or DMSO treatment.

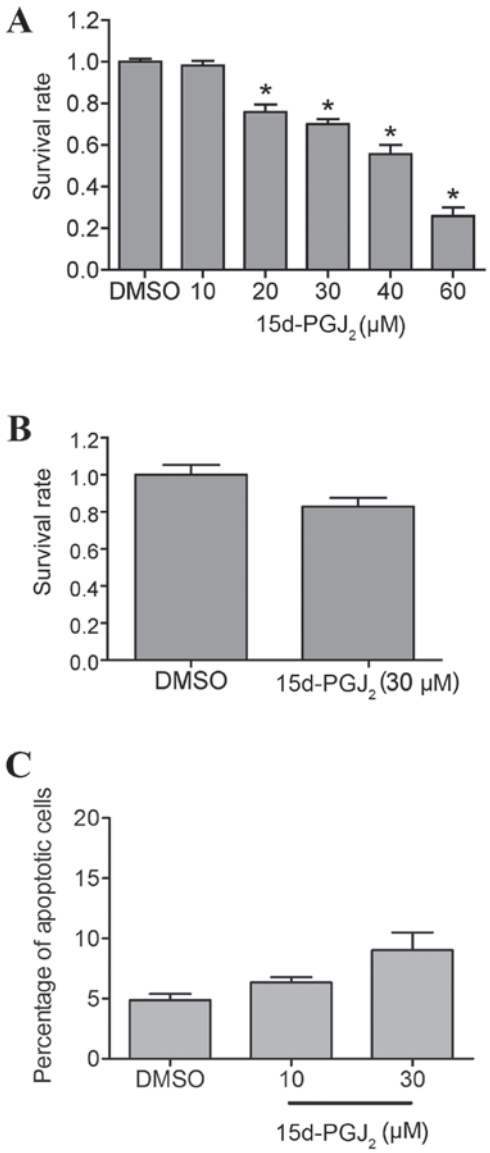

Figure 1. The effect of 15d-PGJ_2 on the viability of human thyroid carcinoma cells. (A) CGTH W-2 cells were treated with DMSO or various concentrations of 15d-PGJ_2 for 24 h and the survival rate was analyzed using an MTT test. *P<0.05 compared with the control group. (B) Rat fibroblasts were treated with DMSO or 30 μM 15dPG2 for 24 h and the survival rate was analyzed using an MTT test. (C) The apoptotic effect of 15d-PGJ_2 on CGTH W-2 cells was assayed using DAPI staining. DMSO, dimethylsulfoxide; 15d-PGJ_2, 15-deoxy-$\Delta^{12,14}$-prostaglandin J_2.

Statistical analysis. All the results are expressed as the mean ± standard deviation. Statistical differences between means were assessed using the Student's t-test in GraphPad Prism (GraphPad Software, Inc., La Jolla, CA, USA). P<0.05 was considered to indicate a statistically significant difference.

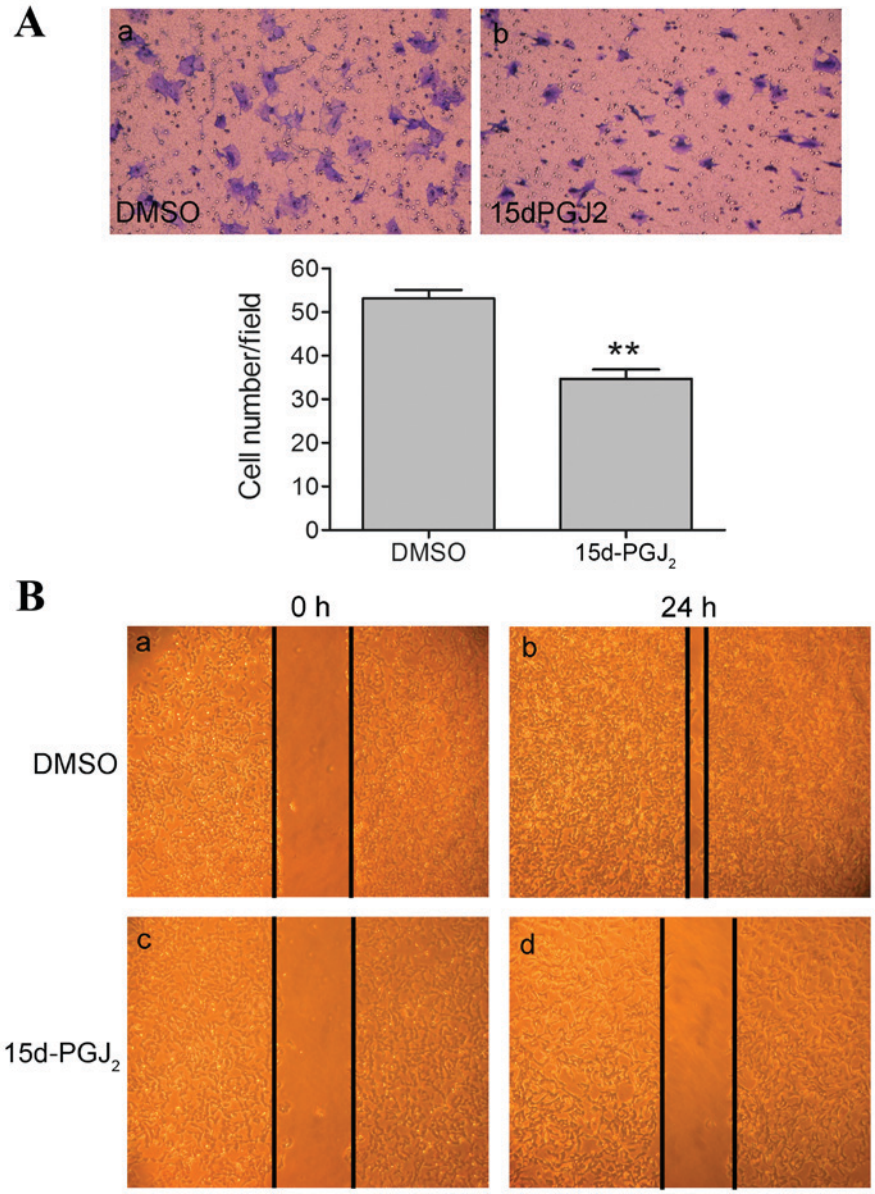

Figure 2. 15d-PGJ$_2$ reduced the level of migration of CGTH W-2 cells. (A) CGTH W-2 cells were seeded in the upper chamber of a Transwell plate. Following 24 h of incubation with or without 30 μM 15d-PGJ$_2$, the number of cells in the lower chamber was calculated. *P<0.05 and **P<0.01, compared with the control group after 24 h. (B) CGTH W-2 cell monolayers were wounded and incubated with or without 30 μM 15dPGJ2 for 24 h. 15d-PGJ$_2$, 15-deoxy-$\Delta^{12,14}$-prostaglandin J$_2$; DMSO, dimethyl sulfoxide.

Results

15d-PGJ$_2$ reduces migration in CGTH W-2 cells. The effect of 15d-PGJ$_2$ on cell viability in human CGTH W-2 thyroid carcinoma cells was evaluated with the MTT assay. The results demonstrated that treatment with 20 and 30 μM 15d-PGJ$_2$ reduced cell viability by 20 and 25%, respectively, compared with untreated CGTH W-2 cells (Fig. 1A) but this was not replicated in rat fibroblasts (Fig. 1B). The survival rate of CGTH W-2 cells declined further with the increased concentration of 15d-PGJ$_2$ (P=0.02, Fig. 1A). Additionally, the reduced survival rate of CGTH W-2 cells was not due to the apoptotic effect by 30 μM 15d-PGJ$_2$ (9%) due to a lack of difference in the percentage of apoptotic cells assayed by nuclear DAPI staining (Fig. 1C).

The effect of 15d-PGJ$_2$ on cell migration was assayed using a Transwell migration and a wound healing assay. Following treatment with 30 μM 15d-PGJ$_2$ for 24 h, the migration rate of thyroid carcinoma cells was significantly reduced by 35% compared with the DMSO control group (P=0.0004, Fig. 2A). The wound healing ability of CGTH W2 cells was also impaired upon treatment with 15d-PGJ$_2$ (Fig. 2B).

15d-PGJ$_2$ decreases cell adhesion in CGTH W-2 cells. The effect of 15d-PGJ$_2$ on the adhesive ability of CGTH W-2 cells was investigated using an adhesion assay. Following a 24 h treatment with 15d-PGJ$_2$, CGTH W-2 cells were plated onto an uncoated or fibronectin-coated dish. As presented in Fig. 3A, 15d-PGJ$_2$ treatment reduced the adhesive ability to 74% of that of the control group (P=0.0075). The current study hypothesized that the adhesion function of integrin was impaired using 15d-PGJ$_2$ treatment as fibronectin is a substrate of integrin (23). The expression levels of proteins in the focal

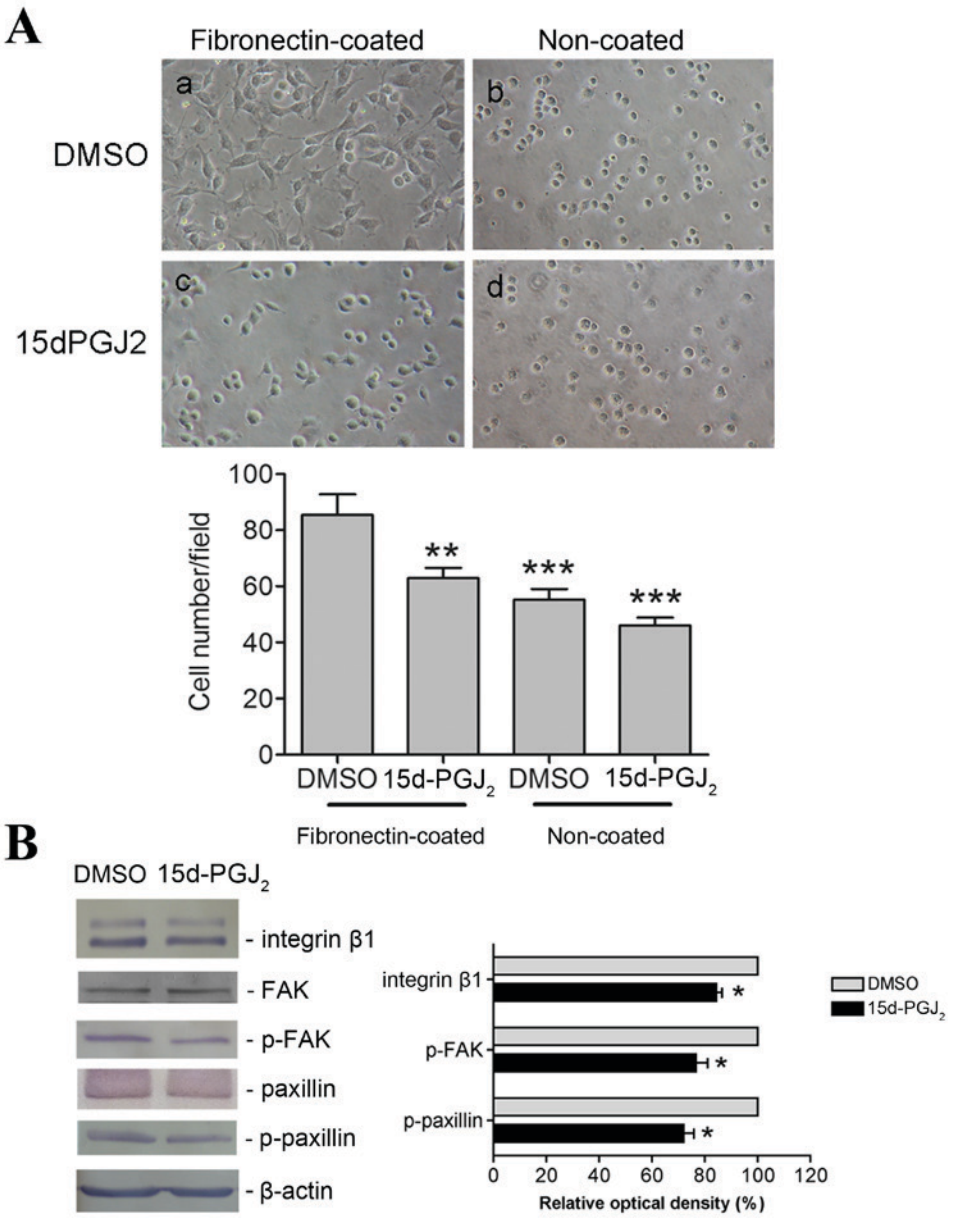

Figure 3. 15d-PGJ_2 impaired cell adhesion and the formation of the focal adhesion complex. (A) The adhesion ability of human thyroid CGTH W-2 cells was assayed. Following 24 h treatment with DMSO or 30 μM 15d-PGJ_2, the cells were detached from the culture dish and re-plated on fibronectin-coated or non-coated dishes for 30 min. **P<0.05 and ***P<0.001, compared with the fibronectin-coated DMSO group after 24 h. (B) Cell lysates were analyzed for the levels of integrin β1, FAK, p-FAK, paxillin and p-paxillin using western blot analysis in CGTH W-2 cells following 15d-PGJ_2 treatment for 24 h. *P<0.05, compared with the DMSO group. 15d-PGJ_2, 15-deoxy-$\Delta^{12,14}$-prostaglandin J_2; DMSO, dimethyl sulfoxide; p-FAK, phosphorylated focal adhesion kinase; p-paxillin, phosphorylated paxillin; FAK, focal adhesion kinase.

adhesion complex were analyzed. This data demonstrated that treatment with 15d-PGJ_2 was significantly associated with the decline of protein expression levels of integrin β1, p-FAK and p-paxillin in CGTH W-2 cells (P=0.04, Fig. 3B). Therefore, 15d-PGJ_2 reduced the adhesive ability of CGTH W-2 thyroid carcinoma cells and this may be due to the reduced phosphorylation of the focal adhesion complex.

The effect of 15d-PGJ_2 on vinculin and actin stress fibers. To understand the distribution of focal adhesion complex proteins and actin stress fibers, CGTH W-2 cells were double stained with vinculin and phalloidin. Following 15d-PGJ_2 treatment, the puncta staining at the periphery and on the ventral side of the cells was decreased, as was the protein staining of vinculin (Fig. 4A). A reduction in the assembly of cortical actin stress fibers was also observed by 30 μM 15d-PGJ_2 treatment (Fig. 4A). The protein expression levels of vinculin were significantly decreased following 15d-PGJ_2 treatment (Fig. 4B).

The distribution of p120-ctn and β-ctn were affected by 15d-PGJ_2. The expression levels and distribution of p120-ctn was examined, as cell lamellipodia and actin stress fibers are reported to be regulated by p120-ctn (10). The CGTH W-2 cells were polygonal and the distribution of p120-ctn was predominantly at the cell junctions. Following 15d-PGJ_2 treatment, membrane ruffles formed at the edge of the cells and p120-ctn accumulated (Fig. 5A). The formation of

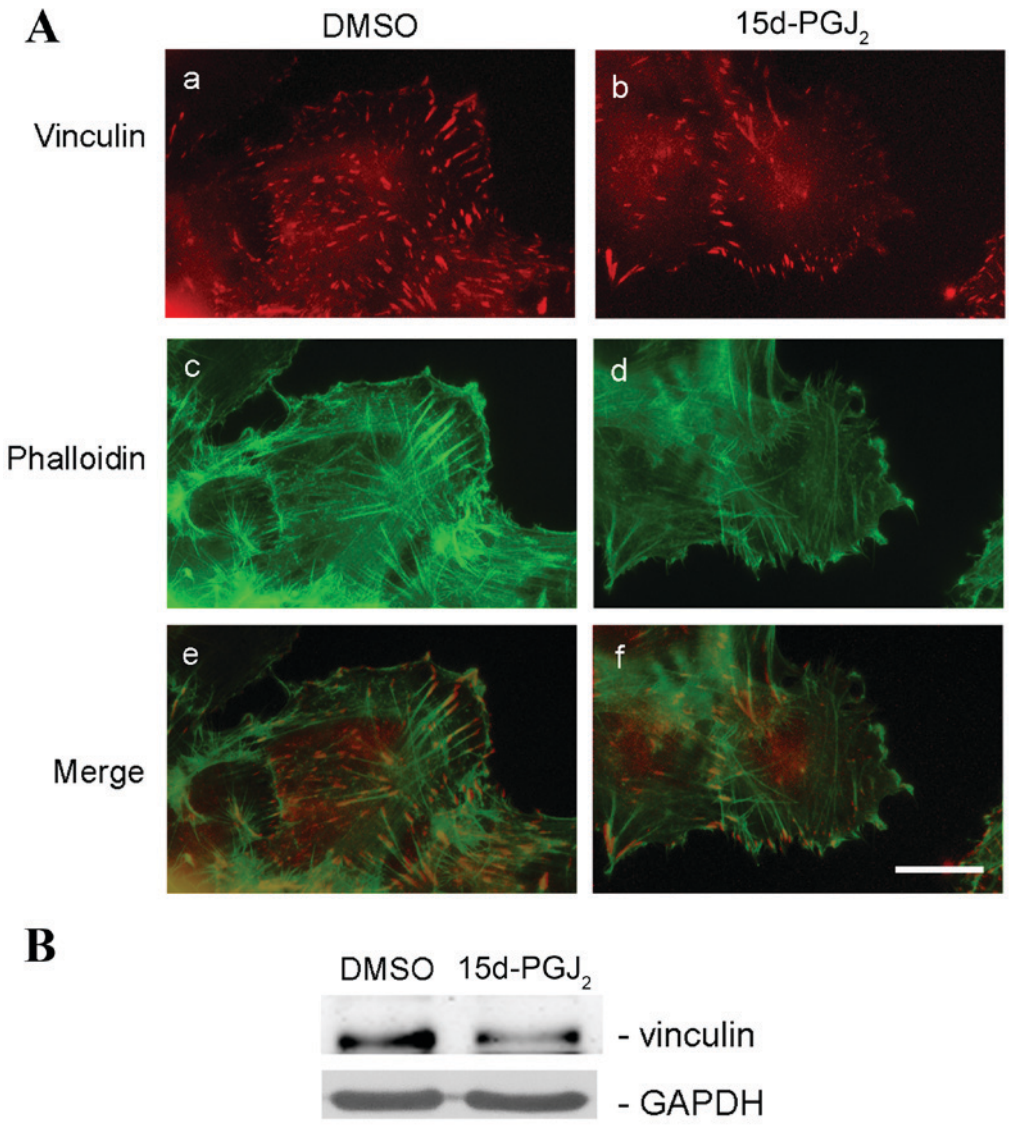

Figure 4. Effects of 15d-PGJ$_2$ on the distributions of vinculin and stress fibers in CGTH W-2 cells. (A) Following a 24 h treatment with 15d-PGJ$_2$ or DMSO treatment, the cells were (a, b) immunostained with vinculin and (c, d) counterstained with fluorescein isothiocyanate-phalloidin. (e, f) These stains were combined to create the merged image. Scale bar=20 μm. (B) Cell lysates were analyzed for vinculin using western blotting in CGTH W-2 cells following 15d-PGJ$_2$ treatment for 24 h. GAPDH was used as a loading control. 15d-PGJ$_2$, 15-deoxy-$\Delta^{12,14}$-prostaglandin J$_2$; DMSO, dimethyl sulfoxide.

lamellipodia and associated protein accumulation were also detected following β-ctn staining (Fig. 5A). The protein expression levels and the distribution of p120-ctn was investigated using western blot analysis. The total protein expression of N-cadherin and p120-ctn were unaffected by 15d-PGJ$_2$ treatment (Fig. 5B). However, N-cadherin and p120-ctn were elevated in the cytosolic portion (P=0.04) and decreased in the membranous portion (P=0.03) following 15d-PGJ$_2$ treatment (Fig. 5C). These data indicate that 15d-PGJ$_2$ may alter the levels of p120-ctn present in the cell membrane compared with p120-ctn levels in the cytoplasm.

Discussion

CGTH W-2 cells lack E-cadherin (12) and therefore, N-cadherin and p120-ctn were investigated to identify the underlying mechanisms of 15d-PGJ$_2$ inhibition in cell migration. Notably, the downregulation of membranous N-cadherin and p120-ctn may lead to a decrease in cell migration in CGTH W-2 cells. Membrane expression levels of p120ctn may control cell spreading and cadherin adhesion (24). Following 15d-PGJ$_2$ treatment, the membranous levels of p120-ctn were reduced, implying that the impairment of cell spreading and adherens junction formation in CGTH W-2 thyroid carcinoma cells may be regulated by p120-ctn. Additionally, cadherin-mediated adhesions may depend on the presence of a functional actin cytoskeleton (24). 15d-PGJ$_2$ treatment was associated with actin disassembly at the ventral section and the periphery of thyroid carcinoma cells, indicating that p120-ctn inhibition may disrupt cadherin-mediated adhesion.

In the majority of tumor cells, N-cadherin displaces E-cadherin during the EMT (25). N-cadherin has several functions that are distinct from the functions of E-cadherin, including fibroblast growth factor receptor 1 activity stimulation, which leads to cell invasion and heterotypic cell-cell adhesions (26). These functions are important for tumor

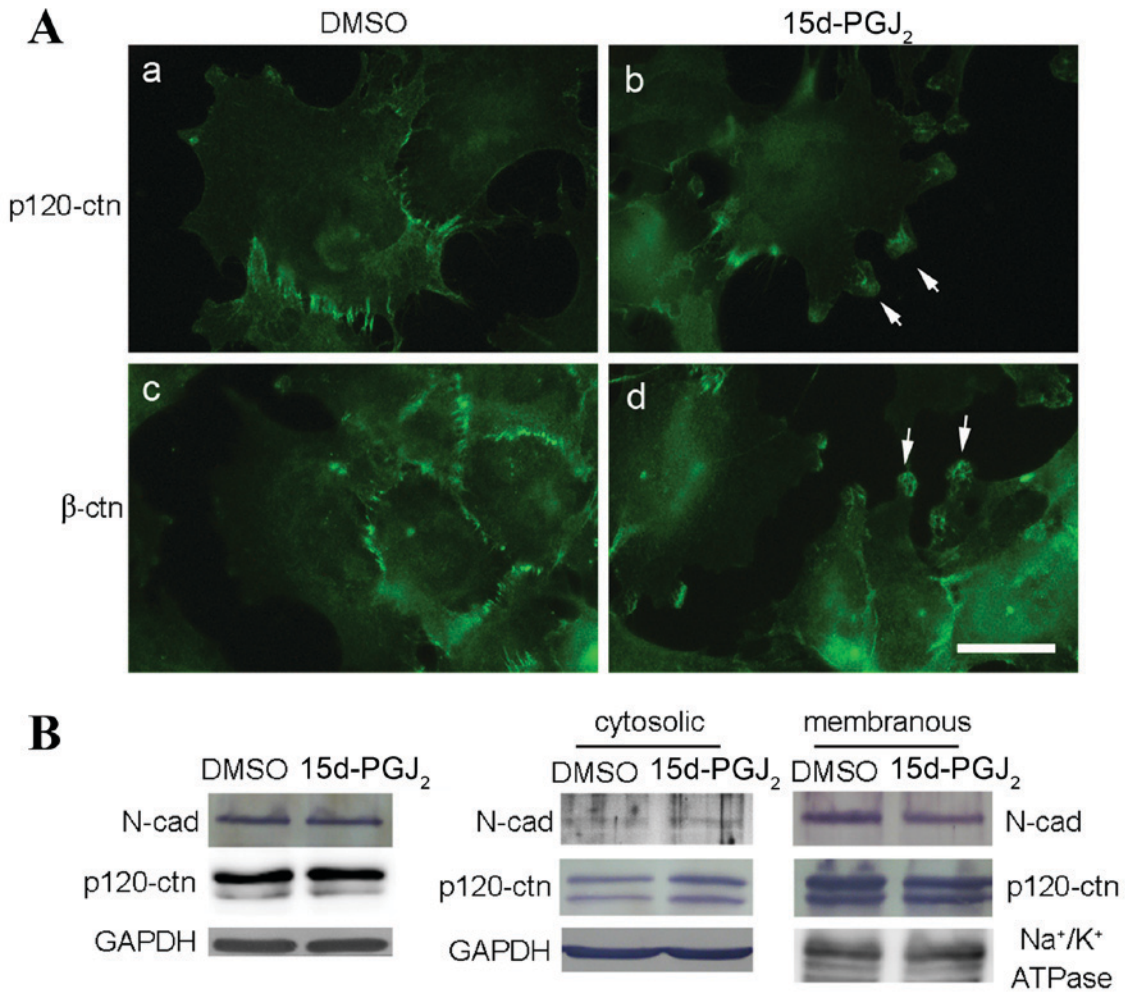

Figure 5. Effects of 15d-PGJ_2 on the distributions of p120-ctn and β-ctn in CGTH W-2 cells. (A) Following 24 h of treatment with 15d-PGJ_2 or DMSO, the cells were immunostained for p120-ctn (a, b) and β-ctn (c, d). Scale bar=20 μm. Arrows indicate lamellipodia at the cell periphery. (B) Cell lysates were analyzed for N-cadherin, p120-ctn expression using western blotting of CGTH W-2 cells following 15d-PGJ_2 or DMSO treatment for 24 h. GAPDH was used as a loading control. (C) Membrane and cytosolic fractions of cell lysates were analyzed for N-cadherin and p120-ctn using western blotting in CGTH W-2 cells following 15d-PGJ_2 or DMSO treatment for 24 h. GAPDH and Na^+/K^+ ATPase were used as loading controls. 15d-PGJ_2, 15-deoxy-$\Delta^{12,14}$-prostaglandin J_2; DMSO, dimethylsulfoxide; p120-ctn, p120-catenin; β-ctn, β-catenin; N-cad, N-cadherin; ATPase, adenosine triphosphatase.

invasion and metastatic dissemination (27). The present study demonstrated that the levels of membrane-associated N-cadherin and cell migration were decreased following treatment with 15d-PGJ_2 , and that the mobility of thyroid carcinoma cells was affected by the PPARγ agonist.

15d-PGJ_2 treatment reduced the survival rate and migration of CGTH W-2 cells, and the reduced cell survival is not accounted for solely by the increase in apoptosis at 30 μM. 15d-PGJ_2 has been reported to suppress proliferation in several cancer cell types, including renal cell, bladder and prostatic carcinoma cells (28). In human bladder carcinoma, 15d-PGJ_2 at a dose of 10 μM for 72 h reduced the cell survival by 90% compared with the control group (29). PPARγ agonists have been reported to block migration in several types of cancer cells (15,30). Pioglitazone, a ligand of PPARγ, suppresses human glioma cell proliferation and migration and triggers glioma cell apoptosis (15). Ciglitazone, a synthetic PPARγ agonist, has been reported to decrease cell migration and invasion in human glioma and melanoma cells via metalloproteinase (MMP)-2 and MMP-9 inactivation and suppression (30). The current study revealed that the reduced cell survival following 15d-PGJ_2 treatment may not be due to apoptosis, but may be associated with the reduction of cell proliferation in CGTH W-2 cells.

A number of previous studies have investigated 15d-PGJ_2 , reporting that it may inhibit cell migration and alter F-actin structure in mouse mammary adenocarcinoma cells (31,32). The current study demonstrates that the migratory and adhesive abilities of human thyroid carcinoma were impaired following 15d-PGJ_2 treatment. The 15d-PGJ_2 treatment reduced the expression levels of focal adhesion proteins, including integrin β1, phosphorylated FAK, phosphorylated paxillin and vinculin, and also decreased the migration and adhesion of CGTH W-2 cells. Additionally the actin stress fibers were altered following 15d-PGJ_2 treatment. Actin filaments are also important to the activation of vinculin, an actin filament binding protein (33).

In conclusion, 15d-PGJ_2 reduced the migration of CGTH W-2 human thyroid carcinoma cells in a Transwell assay and a wound healing assay. The impaired migration may be due to the inactivation of focal adhesion complex, which decreased the cell adhesive ability following 15d-PGJ_2 treatment.

References

1. Huang CJ and Jap TS: A systematic review of genetic studies of thyroid disorders in Taiwan. J Chin Med Assoc 78: 145-153, 2015.
2. Williams D: Thyroid Growth and Cancer. Eur Thyroid J 4: 164-173, 2015.
3. Romitti M, Ceolin L, Siqueira DR, Ferreira CV, Wajner SM and Maia AL: Signaling pathways in follicular cell-derived thyroid carcinomas (review). Int J Oncol 42: 19-28, 2013.
4. Raman P and Koenig RJ: Pax-8-PPAR-γ fusion protein in thyroid carcinoma. Nat Rev Endocrinol 10: 616-623, 2014.
5. Espadinha C, Pinto AE and Leite V: Underexpression of PPARgamma is associated with aneuploidy and lower differentiation of thyroid tumours of follicular origin. Oncol Rep 22: 907-913, 2009.
6. Bonofiglio D, Qi H, Gabriele S, Catalano S, Aquila S, Belmonte M and Andò S: Peroxisome proliferator-activated receptor gamma inhibits follicular and anaplastic thyroid carcinoma cells growth by upregulating p21Cip1/WAF1 gene in a Sp1-dependent manner. Endocr Relat Cancer 15: 545-557, 2008.
7. Aiello A, Pandini G, Frasca F, Conte E, Murabito A, Sacco A, Genua M, Vigneri R and Belfiore A: Peroxisomal proliferator-activated receptor-gamma agonists induce partial reversion of epithelial-mesenchymal transition in anaplastic thyroid cancer cells. Endocrinology 147: 4463-4475, 2006.
8. Husmark J, Heldin NE and Nilsson M: N-cadherin-mediated adhesion and aberrant catenin expression in anaplastic thyroid-carcinoma cell lines. Int J Cancer 83: 692-699, 1999.
9. Kowalewski JM, Shafqat-Abbasi H, Jafari-Mamaghani M, Endrias Ganebo B, Gong X, Strömblad S and Lock JG: Disentangling membrane dynamics and cell migration; differential influences of f-actin and cell-matrix adhesions. PLoS One 10: e0135204, 2015.
10. Van Aken E, De Wever O, Correia da Rocha AS and Mareel M: Defective E-cadherin/catenin complexes in human cancer. Virchows Arch 439: 725-751, 2001.
11. Huang J, Che MI, Huang YT, Shyu MK, Huang YM, Wu YM, Lin WC, Huang PH, Liang JT, Lee PH and Huang MC: Overexpression of MUC15 activates extracellular signal-regulated kinase 1/2 and promotes the oncogenic potential of human colon cancer cells. Carcinogenesis 30: 1452-1458, 2009.
12. Huang SH, Wu JC, Chang KJ, Liaw KY and Wang SM: Distribution of the cadherin-catenin complex in normal human thyroid epithelium and a thyroid carcinoma cell line. J Cell Biochem 70: 330-337, 1998.
13. Ozawa M, Baribault H and Kemler R: The cytoplasmic domain of the cell adhesion molecule uvomorulin associates with three independent proteins structurally related in different species. EMBO J 8: 1711-1717, 1989.
14. Boguslavsky S, Grosheva I, Landau E, Shtutman M, Cohen M, Arnold K, Feinstein E, Geiger B and Bershadsky A: p120 catenin regulates lamellipodial dynamics and cell adhesion in cooperation with cortactin. Proc Natl Acad Sci USA 104: 10882-10887, 2007.
15. Wan Z, Shi W, Shao B, Shi J, Shen A, Ma Y, Chen J and Lan Q: Peroxisome proliferator-activated receptor γ agonist pioglitazone inhibits β-catenin-mediated glioma cell growth and invasion. Mol Cell Biochem 349: 1-10, 2011.
16. Panza A, Pazienza V, Ripoli M, Benegiamo G, Gentile A, Valvano MR, Augello B, Merla G, Prattichizzo C and Tavano F: Interplay between SOX9, β-catenin and PPARγ activation in colorectal cancer. Biochim Biophys Acta 1833: 1853-1865, 2013.
17. Tomar A and Schlaepfer DD: Focal adhesion kinase: Switching between GAPs and GEFs in the regulation of cell motility. Curr Opin Cell Biol 21: 676-683, 2009.
18. Wehrle-Haller B: Assembly and disassembly of cell matrix adhesions. Curr Opin Cell Biol 24: 569-581, 2012.
19. Hauck CR, Hsia DA and Schlaepfer DD: The focal adhesion kinase-a regulator of cell migration and invasion. IUBMB Life 53: 115-119, 2002.
20. Chen Y, Wang SM, Wu JC and Huang SH: Effects of PPARgamma agonists on cell survival and focal adhesions in a Chinese thyroid carcinoma cell line. J Cell Biochem 98: 1021-1035, 2006.
21. Lin JD, Chao TC, Weng HF, Huang HS and Ho YS: Establishment of xenografts and cell lines from well-differentiated human thyroid carcinoma. J Surg Oncol 63: 112-118, 1996.
22. de Amicis F, Lanzino M, Kisslinger A, Calì G, Chieffi P, Andò S, Mancini FP and Tramontano D: Loss of proline-rich tyrosine kinase 2 function induces spreading and motility of epithelial prostate cells. J Cell Physiol 209: 74-80, 2006.
23. Tharmalingam S, Daulat AM, Antflick JE, Ahmed SM, Nemeth EF, Angers S, Conigrave AD and Hampson DR: Calcium-sensing receptor modulates cell adhesion and migration via integrins. J Biol Chem 286: 40922-40933, 2011.
24. Gavard J, Lambert M, Grosheva I, Marthiens V, Irinopoulou T, Riou JF, Bershadsky A and Mège RM: Lamellipodium extension and cadherin adhesion: Two cell responses to cadherin activation relying on distinct signalling pathways. J Cell Sci 117: 257-270, 2004.
25. Chiang KC, Kuo SF, Chen CH, Ng S, Lin SF, Yeh CN, Chen LW, Takano M, Chen TC, Juang HH, *et al*: MART-10, the vitamin D analog, is a potent drug to inhibit anaplastic thyroid cancer cell metastatic potential. Cancer Lett 369: 76-85, 2015.
26. van Roy F: Beyond E-cadherin: Roles of other cadherin superfamily members in cancer. Nat Rev Cancer 14: 121-134, 2014.
27. Abolhassani A, Riazi GH, Azizi E, Amanpour S, Muhammadnejad S, Haddadi M, Zekri A and Shirkoohi R: FGF10: Type III epithelial mesenchymal transition and invasion in breast cancer cell lines. J Cancer 5: 537-547, 2014.
28. Yoshimura R, Matsuyama M, Hase T, Tsuchida K, Kuratsukuri K, Kawahito Y, Sano H, Segawa Y and Nakatani T: The effect of peroxisome proliferator-activated receptor-gamma ligand on urological cancer cells. Int J Mol Med 12: 861-865, 2003.
29. Chaffer CL, Thomas DM, Thompson EW and Williams ED: PPARgamma-independent induction of growth arrest and apoptosis in prostate and bladder carcinoma. BMC Cancer 6: 53, 2006.
30. Papi A, Rocchi P, Ferreri AM, Guerra F and Orlandi M: Enhanced effects of PPARγ ligands and RXR selective retinoids in combination to inhibit migration and invasiveness in cancer cells. Oncol Rep 21: 1083-1089, 2009.
31. Diers AR, Dranka BP, Ricart KC, Oh JY, Johnson MS, Zhou F, Pallero MA, Bodenstine TM, Murphy-Ullrich JE, Welch DR and Landar A: Modulation of mammary cancer cell migration by 15-deoxy-delta(12,14)-prostaglandin J (2): Implications for anti-metastatic therapy. Biochem J 430: 69-78, 2010.
32. Schell C, Albrecht M, Spillner S, Mayer C, Kunz L, Köhn FM, Schwarzer U and Mayerhofer A: 15-Deoxy-delta 12-14-prostaglandin-J2 induces hypertrophy and loss of contractility in human testicular peritubular cells: Implications for human male fertility. Endocrinology 151: 1257-1268, 2010.
33. Chen H, Choudhury DM and Craig SW: Coincidence of actin filaments and talin is required to activate vinculin. J Biol Chem 281: 40389-40398, 2006.